Solar/interplanetary plasma phenomena causing geomagnetic activity at Earth

B.T. TSURUTANI

Jet Propulsion Laboratory - Pasadena, California

Summary. — Solar wind phenomena leading to different types of geomagnetic activity are discussed. The solar and interplanetary causes and the physical processes leading to: magnetic storms, substorms, geomagnetic quiet and the dayside aurora will be reviewed. Some plasma processes leading to auroras will be discussed.

PACS 94.30 – Physics of the magnetosphere.
PACS 96.50 – Interplanetary space.

1. – Introduction

There are a variety of different physical mechanisms responsible for transferring solar wind energy and momentum into the Earth's magnetosphere. The dominant mechanism for magnetic storms and substorms is generally agreed to be magnetic reconnection, interconnection between interplanetary and planetary fields. For lesser intensity geomagnetic activities, there are numerous other mechanisms. One of these, cross-field diffusion due to resonant wave-particle interactions will be addressed in detail.

Plasma instabilities within the Earth's magnetosphere lead to electromagnetic and electrostatic wave growth, concomitant particle pitch angle scattering, and loss of particles into the ionosphere. Ionospheric atoms and molecules excited by the precipitating

particles quickly decay, giving off the characteristic aurora borealis (northern lights) and aurora australis (southern lights) near the magnetic poles.

The purpose of this paper is to briefly review the mechanisms for injecting anisotropic plasmas into the magnetosphere. For a review of magnetosphere plasma processes, we suggest articles in "From the Sun: Auroras, magnetic storms, solar flares, cosmic rays" by Suess and Tsurutani [1]. A review of magnetic storms can be found in Gonzalez *et al.* [2].

2. – Magnetic Reconnection

A schematic for magnetic reconnection at Earth is shown in Fig. 1. The magnetic field of the Earth has its south magnetic pole in the north and vice-versa. Thus, the sunward side of the magnetopause has magnetic fields that are directed from south-to-north. Because magnetic reconnection occurs between oppositely directed fields, a southwardly oriented interplanetary magnetic field will interconnect with the Earth's magnetic field at the magnetopause nose.

The solar wind normally flows radially outward with speeds of ~400 km s^{-1}. The solar wind plasma β ($8\pi nkT/B^2$) is ~1.0. After reconnection, the embedded, connected, magnetospheric fields are dragged in the antisolar direction by the solar wind. The fields reconnect in the tail and the magnetic tension convects the fields and plasma towards the nightside of the Earth. The plasma is betatron accelerated by the above convection, increasing the temperature/energy of the plasma in the component perpendicular to $\vec{B}$.

3. – Particle motions, plasma instabilities

After the plasma is convected into the dipolar magnetic field regions of the Earth's magnetosphere, the ions and electrons are subjected to the conservation of three adiabatic invariants involving the particle cyclotron, bounce and drift motions. These particle motions are illustrated in Fig. 2. The Earth's magnetic field is essentially a magnetic bottle with the two ends of the bottle in the northern and southern hemispheric ionospheres. Particles gyrate about the magnetic field in a cyclotron motion. Particles with pitch angles other than 90° "bounce" between their two mirror points. Magnetic field gradients and field curvature lead to azimuthal drift. Protons and other ions drift from midnight towards dusk, and electrons drift from midnight towards dawn. Thus, a ring of current (called the "ring current") is formed.

The plasma temperature anisotropies created by the nightside inward convection lead to a "loss-cone" instability and growth of plasma waves. A type of electromagnetic wave, called chorus, is shown in Fig. 3. These waves propagate in the whistler mode. The waves resonantly interact with electrons and pitch angle scatter them towards isotropy. Particles scattered into the "loss cone" will have their mirror points lowered to deep within the ionosphere/atmosphere. These electrons lose their kinetic energy via collisions with atoms and molecules, and they do not return to the magnetosphere. Most of the precipitating energetic particle energy goes into atomic and molecular excitation, and

with subsequent decay, characteristic photons are emitted which define the aurora. Only a small amount of the energy is emitted in bremsstrahling x-rays.

Besides the aurora, there are other signatures of magnetic storms and substorms (from the term "substorms" it is clear that they were originally thought to be a fundamental element of a magnetic storm [3]). For magnetic storms, there are magnetic deviations measured at Earth due to the enhanced ring current (discussed earlier). This current is a diamagnetic one and thus it causes decreases in the horizontal component of the Earth's field, measured at the equator. The 1989 "great" storm was particularly large, with a maximum decrease of -589 nT. The Earth's magnetic field at the equator is $\sim 0.3 \times 10^5$ nT. Thus for this event, the geomagnetic field change at the surface of the Earth was on the order of $\sim 2\%$. The phase of a storm where the ring-current is growing is called the "main phase" (shown in Fig. 4). The loss of ring current particles (by charge exchange, Coulomb scattering and wave-particle interactions) defines the recovery phase [4]. The loss rate is dependent on the particle's pitch angle, energy, and location relative to the Earth. The general time scale is typically hours.

4. – Magnetic storms

During solar maxima, fast ejecta coming from the Sun are often preceded by a forward shock. The high velocities ($\sim$600 to 1000 km s^{-1}) and the high densities (an increase from a nominal 5 cm^{-3} to 10-20 cm^{-3}) at the shock are associated with a very large solar wind ram pressure increase. This solar wind compression of the magnetosphere (pressure balance is obtained) causes the "initial phase" of the storm (Fig. 4) detected at Earth.

There are several sources for the southward interplanetary fields leading to magnetic reconnection. During solar maximum, fast interplanetary coronal mass ejections (ICMEs) and their associated upstream shocks and sheaths are the primary cause. The two primary regions that contain intense magnetic fields (which may or may not be southward oriented) is the sheath region between the shock and the solar ejecta proper, and also the ejecta itself. A schematic of this is shown in Fig. 5. The Sun is on the left.

Figure 6 shows an interplanetary event where part of the solar ejecta had a strong southward field. Note as the B_Z component turns negative (southward), the ring-current increases (D_{ST} decreases). This is an empirical confirmation of the reconnection mechanism. The D_{ST} decrease profile is similar to the negative B_Z profile.

Figure 7 illustrates a case where interplanetary sheath B_S fields lead to the ring-current/storm main phase. The fields upstream of the shock are oriented southward. The shock compresses this field, leading to intensified B_S, and presumably intensified magnetic reconnection.

5. – Substorms

In the declining phase of the solar cycle, the main cause of geomagnetic activity is corotating streams. Ulysses determined that high-speed (750-800 km s^{-1}), continuous

streams emanate from coronal holes [5]. The streams contain large amplitude nonlinear Alfvén waves propagating away from the Sun [6] [7].

These high-speed streams overtake slower speed streams. At the interaction interface, the magnetic field is compressed and the plasma density and temperatures are enhanced. This interaction region has been called a corotating interaction region (CIR), because it "corotates" with the Sun. An example is shown in Fig. 8. The B_Z field component within the CIR is highly fluctuating. Note that the magnetic storm amplitude (D_{ST}) is correspondingly smaller than previous examples, and irregular in form.

There is typically no forward shock leading the CIR at 1 AU. Shocks are generally formed much farther from the Sun [8]. The slower speed stream contains high density plasma. The compression due to the high-speed stream interaction leads to a further density intensification. Thus, the high-density (low speed) region causes increased ram pressure as it impinges on the magnetosphere, causing the storm "initial phase". Large amplitude Alfvén waves are present in the high speed stream proper. The transverse fluctuations are assumed to be random in direction. However, when the B_Z component turns southward, magnetic reconnection occurs and, after some delay, the ionospheric auroral electrojet intensifies (an indication of a substorm). Figure 9 shows an example of this. There is a sequence of southward turnings of the interplanetary magnetic field B_Z component, and a corresponding set of AE (auroral electrojet index) increases.

Substorms occur primarily in the midnight sector of the magnetosphere. The process is similar to that of magnetic storms (for a discussion of the substorm-storm relationship, see Kamide *et al.* [9]). There is particle injection from the tail region, but the intensity of the plasma injection is much smaller than for storms. There is correspondingly a small increase in the ring current (a D_{ST} decrease) with each substorm.

A continuous series of auroral substorms is called a High Intensity Long-Duration Continuous Auroral Activity (HILDCAA) event. Because the high-speed stream (and Alfvén waves) occur just sunward (later in time) of the corotating interaction region, HILDCAAs occur after the small storm caused by the CIR. Thus the continuing activity, which is associated with small plasma injections, makes it appear as if the ring current decays quite slowly (the substorm intensities abate gradually due to the gradual decrease in Alfvén wave amplitudes). In actuality, a HILDCAA event represents a series of pulsed plasma injections, so the apparent long decay is really due to additional injection events with diminishing intensities [10].

It has recently been shown that during 1974, HILDCAAs associated with two corotating high-speed streams led to an average auroral energy higher than during 1979, a year of solar maximum [10].

6. – Geomagnetic quiet

Geomagnetic quiet refers to the absence of magnetic storms and large substorms. The interplanetary causes of geomagnetic quiet are different during different phases of the solar cycle. During solar maximum, intense northwardly directed interplanetary magnetic fields and the lack of magnetic reconnection lead to an energy input into the

magnetosphere 100 to 30 times less than periods of intense southward fields [11]. The intense northward fields are often found in ICMEs. During the declining phase of the solar cycle, the far trailing portion of high-speed streams/beginning of the heliospheric current sheet plasma sheet [12] is characterized by low field intensities (3-5 nT), low solar wind speeds (< 350 km s^{-1}) and an absence of field fluctuations. These conditions also lead to geomagnetic quiet [10]. Although the interplanetary conditions for these two cases are quite different, one common feature is the lack of southward fields, and thus, geomagnetic quiet.

7. – Dayside aurora

It was previously mentioned that plasma gets injected into the nightside magnetosphere during storms and substorms. The injections and the instabilities leading to particle precipitation and auroras in the midnight sector are episodic (however during storms, the particles eventually spread throughout the magnetosphere).

In contrast, there are also auroras on the dayside. This latter phenomenon is at lower intensity levels than that in the nightside, and is a more-or-less ever-present feature of the dayside ionosphere. What physical process creates this aurora? There have been a number of theoretical ideas suggested. I will review one particular mechanism, that of cross-field diffusion.

Figure 10 illustrates ion fluxes in the magnetopause boundary layer [13]. The solar wind consists primarily of protons with $\sim 4\%$ He^{++} ions. There are also trace amounts of highly ionized carbon, nitrogen and oxygen ions present. These minor ions are extremely useful in identifying the origins of the plasma. In Fig. 10, the He^{++} and CNO group ion flux levels are high in the sheath behind the Earth's bow shock and they decreases gradually across the boundary layer. Clearly, the ions are being diffused across magnetic field lines.

Singly ionized oxygen and helium ions have an ionospheric source. Processes (not described) have led to their energization to the 10s of keV energy range (and higher). These particles are present in the magnetosphere. In Fig. 10, O^+ and He^+ ion fluxes are high in the magnetosphere and decrease across the boundary layer. These ions are being diffused outward.

Plasma waves are detected in the magnetopause boundary layer (Fig. 11) which have both electric and magnetic components. The waves have apparent broad band spectra and are believed to be electromagnetic whistler mode plus electrostatic waves [14] [15]. Recent results [16] indicate that the "electrostatic component" may be due mainly to discrete "electron hole" events.

The Pederson mobility of particles in a direction perpendicular to B_0 is given as

$$\mu_\perp = \frac{c}{B_0} \frac{\Omega\tau_{eff}}{(\Omega\tau_{eff})^2}$$

[17]. From Rose and Clark [18], we have an expression for cross-field transport

$$D_\perp = \frac{E_\perp c}{eB_0} \frac{\Omega\tau_{eff}}{1+(\Omega\tau_{eff})^2}$$

where c is the speed of light, Ω the cyclotron frequency, e the particle charge, and τ_{eff} the effective collision time.

Assuming cyclotron resonant interactions between waves and particles in the boundary layer, the pitch angle scattering diffusion is given as

$$D^{\pm}_{\alpha\alpha} \cong (\frac{B_\omega}{B_0})^2 \Omega^{\pm}$$

$$D^{\pm}_{\alpha\alpha} \cong (\frac{c}{v})^2 (\frac{E_\omega}{B_0})^2 \Omega^{\pm}$$

for magnetic and electric wave components, respectively [19]. Tsurutani and Thorne [20] have derived an expression for cross-field diffusion, assuming that the effective collision time is much larger than Ω^{-1}. They obtained:

$$D_{\perp B_\omega} \cong 2(\frac{B_\omega}{B_0})^2 D_{max}$$

$$D_{\perp E_\omega} \cong 2(\frac{c}{v})(\frac{E_\omega}{B_0})^2 D_{max}$$

where D_{max}, the Bohm diffusion rate, is defined as $E_\perp c/2eB_0$.

Representative magnetosheath values were applied and it was shown that the waves had sufficient intensity to cause rapid diffusion of magnetosheath plasma into the magnetosphere and the formation of the boundary layer at the Earth's magnetopause. Using the measured particle fluxes in the boundary layer, it was found that the pitch angle diffusion rates for electrons and protons were near the strong diffusion limit. The calculated fluxes were shown to be sufficient to create the dayside aurora (~ 1 erg cm^{-2} s^{-1}).

* * *

Portions of this work were done at the Jet Propulsion Laboratory, California Institute of Technology under contract with National Aeronautics and Space Administration.

REFERENCES

[1] SUESS S.T. and TSURUTANI B.T., *From the Sun: Auroras, Magnetic Storms, Solar Flares, Cosmic Rays*, (Am. Geophys. Union, Washington D.C.) 1998.

[2] GONZALEZ W.D., JOSELYN J.A., KAMIDE Y., KROEHL H.W., ROSTOKER G., TSURUTANI B.T. and VASYLIUNAS V.M., *What is a geomagnetic storm?*, *J. Geophys. Res.*, **99** (1994) 5771

[3] AKASOFU S.-I., *The development of the auroral substorm*, *Planet. Space Sci.*, **12** (1964) 273

[4] KOZYRA J.U., JORDANOVA V.K., HORNE R.B., and THORNE R.M., *Modeling of the contribution of electromagnetic ion cyclotron (EMIC) waves to stormtime ring current erosion*, in *Magnetic Storms*, edited by TSURUTANI B.T., GONZALEZ W.D., KAMIDE Y. and ARBALLO J.K. (Am. Geophys. Union, Washington D.C.) 1997, pp. 187-202.

[5] PHILLIPS J.L., BALOGH A., BAME S.J., GOLDSTEIN B.E., GOSLING J.T., HOEKSEMA J.T., MCCOMAS D.J., NEGEBAUER M., SHEELEY N.R. JR. and WANG Y.M., *Ulysses at 50° south: Constant immersion in the high speed solar wind*, *Geophys. Res. Lett.*, **21** (1994) 1105

[6] TSURUTANI B.T., HO C.M., SMITH E.J., NEUGEBAUER M., GOLDSTEIN B.E., MOK J.S., ARBALLO J.K., BALOGH A., SOUTHWOOD D.J. and FELDMAN W.C., *The relationship between interplanetary discontinuities and Alfvén waves: Ulysses observations, Geophys. Res. Lett.*, **21** (1994) 2267

[7] BALOGH A., SMITH E.J., TSURUTANI B.T., SOUTHWOOD D.J., FORSYTH R.J. and HORBURY T.S., *The heliospheric magnetic field over the south polar region of the Sun, Science*, **268** (1995) 1007

[8] SMITH E.J. and WOLFE J.W., *Observations of interaction regions and corotating shocks between one and five AU: Pioneers 10 and 11, Geophys. Res. Lett.*, **3** (1976) 137

[9] KAMIDE Y., BAUMJOHANN W., DAGLIS I.A., GONZALEZ W.D., GRANDE M., JOSELYN J.A., MCPHERRON R.L., PHILLIPS J.L., REEVES E.G.D., ROSTOKER G., SHARMA A.S., SINGER H.J., TSURUTANI B.T. and VASYLIUNAS V.M., *Current understanding of magnetic storms; storm/substorm relationships, J. Geophys. Res.*, **103** (1998) 17705

[10] TSURUTANI B.T., GONZALEZ W.D., GONZALEZ A.L.C., TANG F., ARBALLO J.K. and OKADA M., *Interplanetary origin of geomagnetic activity in the declining phase of the solar cycle, J. Geophys. Res.*, **100** (1995) 21717

[11] TSURUTANI B.T. and GONZALEZ W.D., *The efficiency of "viscous interaction" between the solar wind and the magnetosphere during intense northward IMF events, Geophys. Res. Lett.*, **22** (1995) 663

[12] WINTERHALTER D., SMITH E.J., BURTON M.E., MURPHY N. and MCCOMAS D.J., *The heliospheric plasma sheet, J. Geophys. Res.*, **99** (1994) 6667

[13] EASTMAN T. and CHRISTON S., *Ion composition and transport near the Earth's magnetopause*, in *Physics of the Magnetopause*, edited by SONG P., SONNERUP B.U.Ö. and THOMSEN M.F. (Am. Geophys. Union, Washington D.C.) 1995, pp. 131-137.

[14] GURNETT D.A., ANDERSON R.R., TSURUTANI B.T., SMITH E.J., PASCHMANN G., HAERENDEL G., BAME S.J. and RUSSEL C.T., *Plasma wave instabilities at the magnetopause: Observations from ISEE 1 and 2, J. Geophys. Res.*, **84** (1979) 7043

[15] TSURUTANI B.T., LAKHINA G.S., HO C.M., ARBALLO J.K., GALVAN C., BOONSIRISETH A., PICKETT J.S., GURNETT D.A., PETERSON W.K. and THORNE R.M., *Broadband plasma waves observed in the polar cap boundary layer: Polar, J. Geophys. Res.*, **103** (1998) 17351

[16] TSURUTANI B.T., ARBALLO J.K., LAKHINA G.S., HO C.M., BUTI B., PICKETT J.S. and GURNETT D.A., *Plasma waves in the dayside polar cap boundary layer: Bipolar and monopolar electric pulses and whister mode waves, Geophys. Res. Lett.*, **25** (1998) 4117

[17] SCHULZ M. and LANZEROTTI L.J., *Particle Diffusion in the Radiation Belts*. (Springer-Verlag, New York) 1974.

[18] ROSE D.J. and CLARK M., *Plasma and Controlled Fusion*, (John Wiley, New York) 1961.

[19] KENNEL C.F. and PETSCHEK H.E., *Limit on stably trapped particle fluxes, J. Geophys. Res.*, **71** (1966) 1

[20] TSURUTANI B.T. and THORNE R.M., *Diffusion processes in the magnetopause boundary layer, Geophys. Res. Lett.*, **9** (1982) 1247

APPENDIX A.

Figure captions

Fig. 1. - A schematic of magnetic reconnection between interplanetary magnetic fields and magnetospheric fields. This process leads to plasma injection into the nightside magnetosphere.
Fig. 2. - Charged particle motion in the Earth's magnetic fields.
Fig. 3. - An example of electromagnetic "chorus" waves generated by the electron loss cone instability.
Fig. 4. - The three phases of a magnetic storm: initial, main, and recovery. The storm profiles and causes are different during solar maximum and solar minimum. Magnetic deviations due to the ring current can be $\sim 1 - 2\%$ of the Earth's field.
Fig. 5. - A schematic of an interplanetary coronal mass ejection (ICME) plus upstream shock and sheath.
Fig. 6. - An ICME event with an embedded magnetic cloud. The magnetic cloud's southward fields lead to the storm main phase through the magnetic reconnection process. The interplanetary shock is denoted by an "S".
Fig. 7. - Interplanetary shock/sheath fields that lead to a storm main phase.
Fig. 8. - A fast stream-slow stream interaction: compressed magnetic fields. Due to the high variability in B_Z, this CIR causes only a minor magnetic storm.
Fig. 9. - Large amplitude Alfvén wave B_S fluctuations causing substorms (AE increases) and small ring current increases (D_{ST} decreases).
Fig. 10. - Diffusion of magnetosheath and magnetospheric ions across the magnetopause boundary layer.
Fig. 11. - Plasma waves within the magnetopause boundary layer.

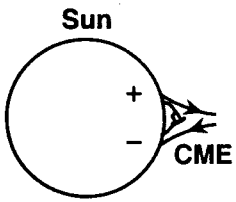

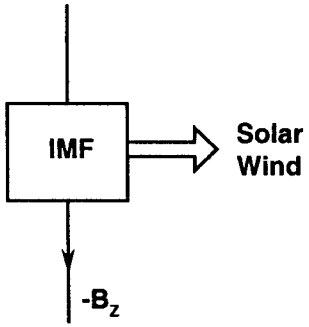

IMF: Interplanetary Magnetic Field

B_z: Southward component of IMF

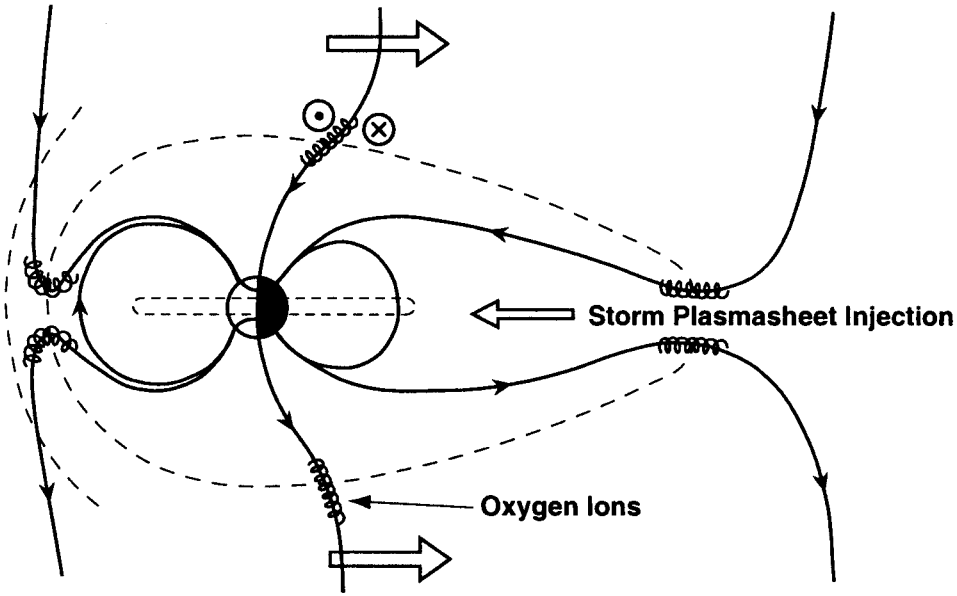

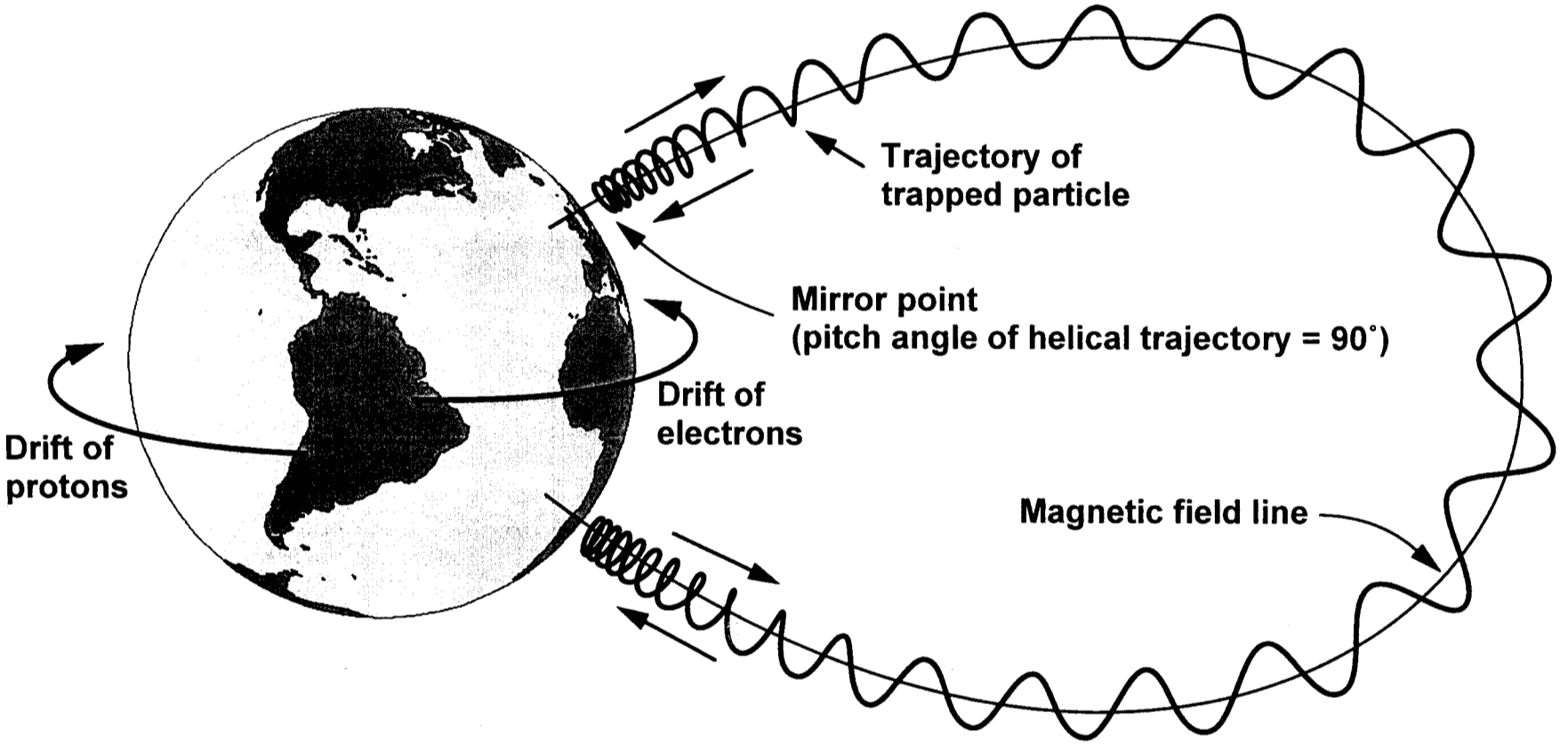
Trajectory of
trapped particle
Mirror point
(pitch angle of helical trajectory = 90˚)
Drift of
electrons
Drift of
protons
Magnetic field line

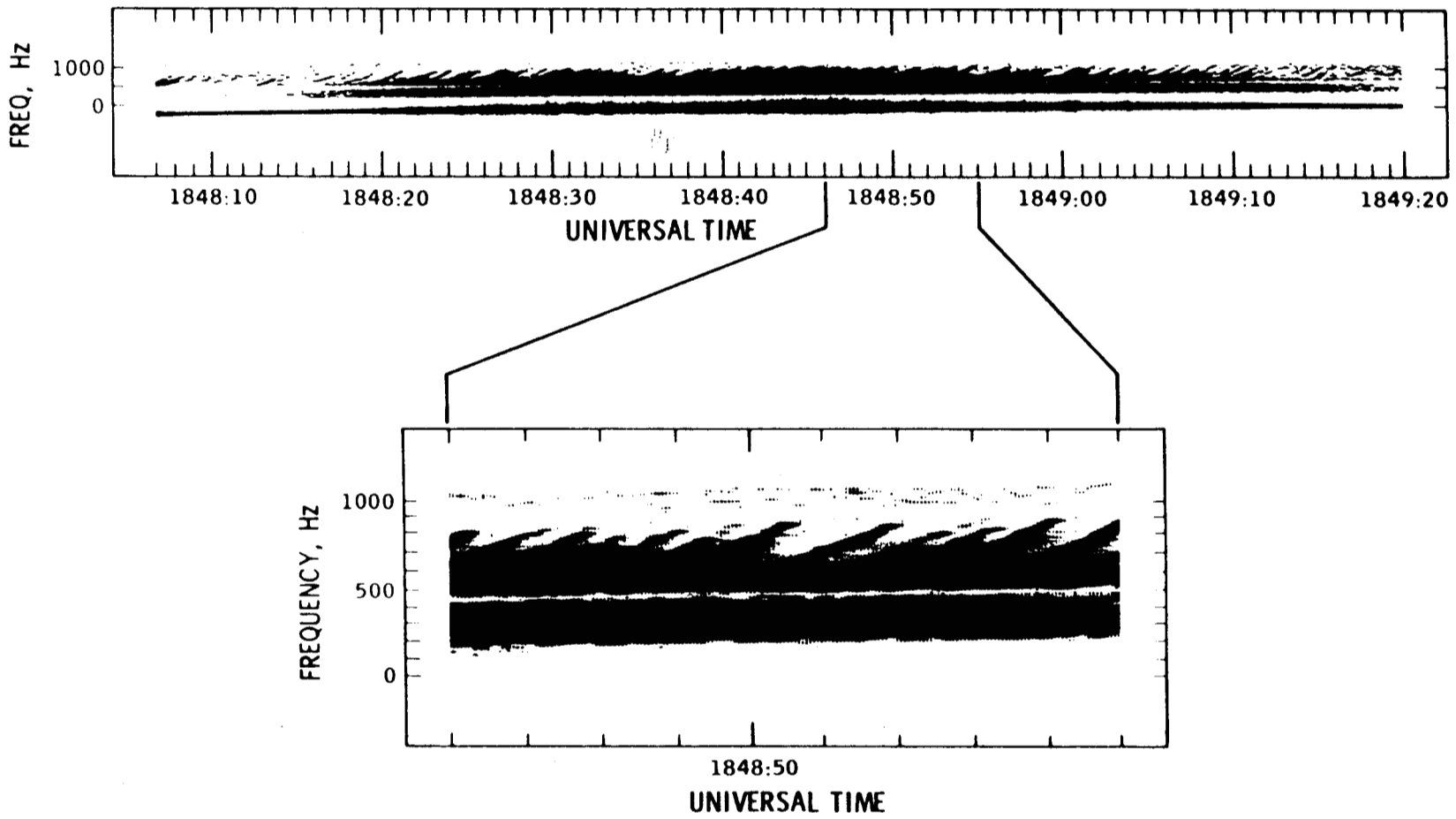

OGO-5 REV 132
FEBRUARY 10, 1969
1251 LOCAL TIME

MLAT = -8.0°
L = 7.9
P = 70γ

Solar Maximum (ICME) Storm

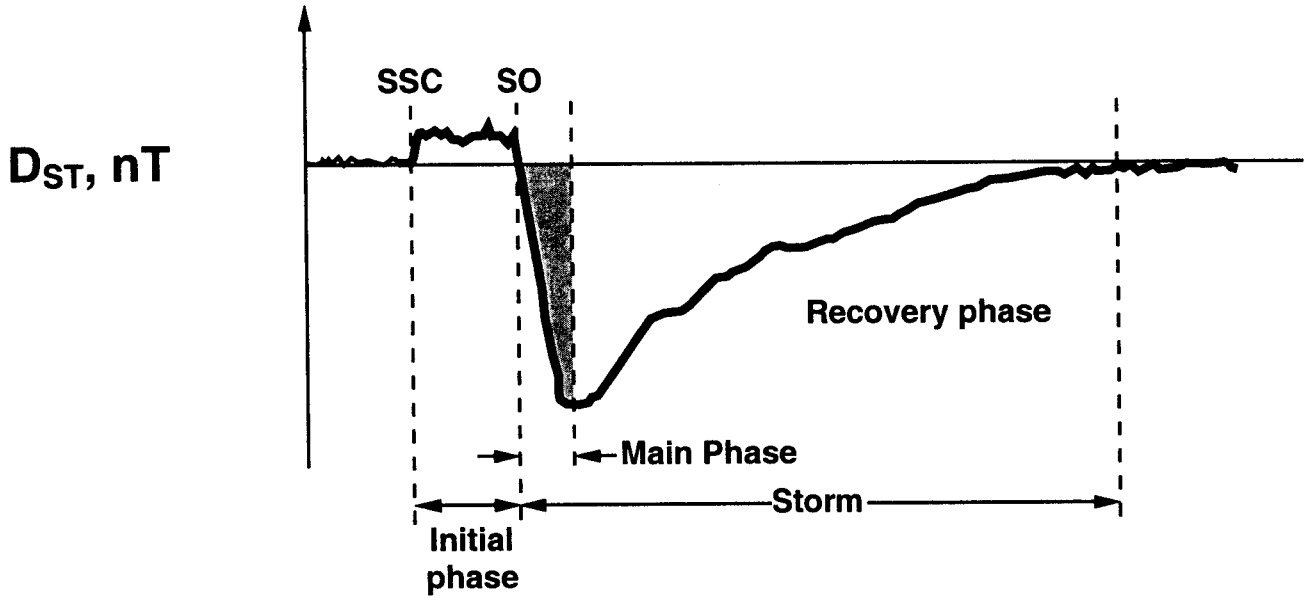

Solar Minimum (CIR) Storm

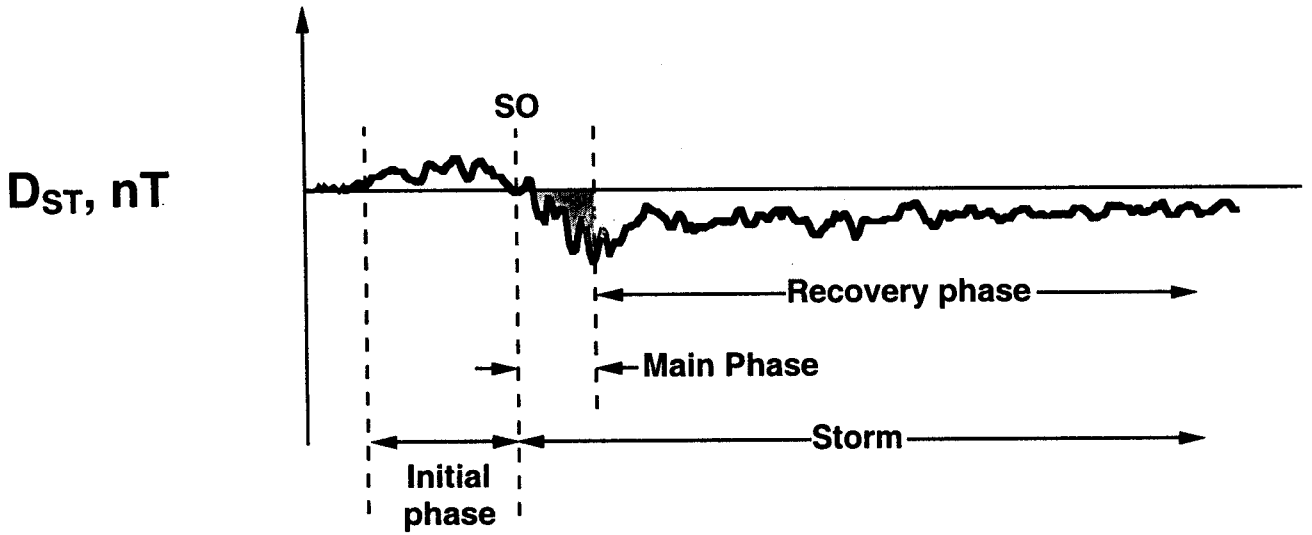

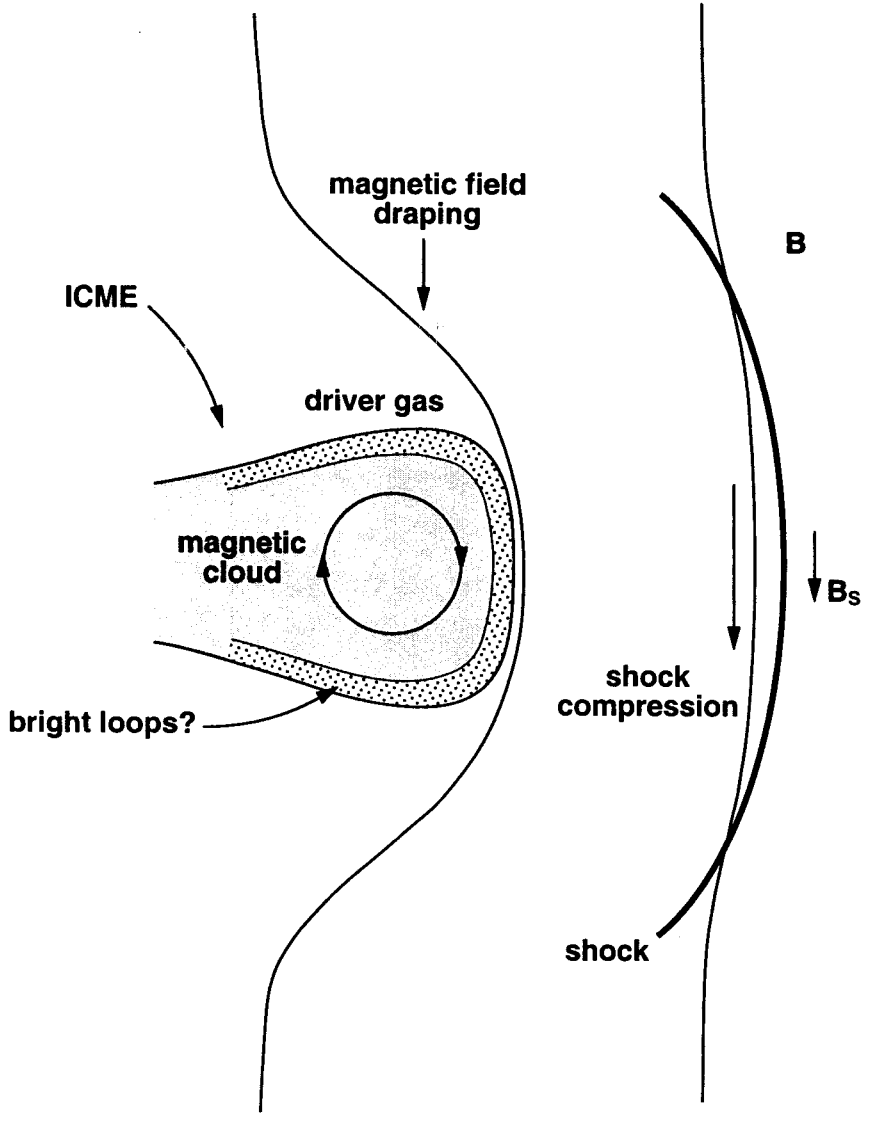
magnetic field
draping
ICME
driver gas
magnetic
cloud
bright loops?
B
B_S
shock
compression
shock

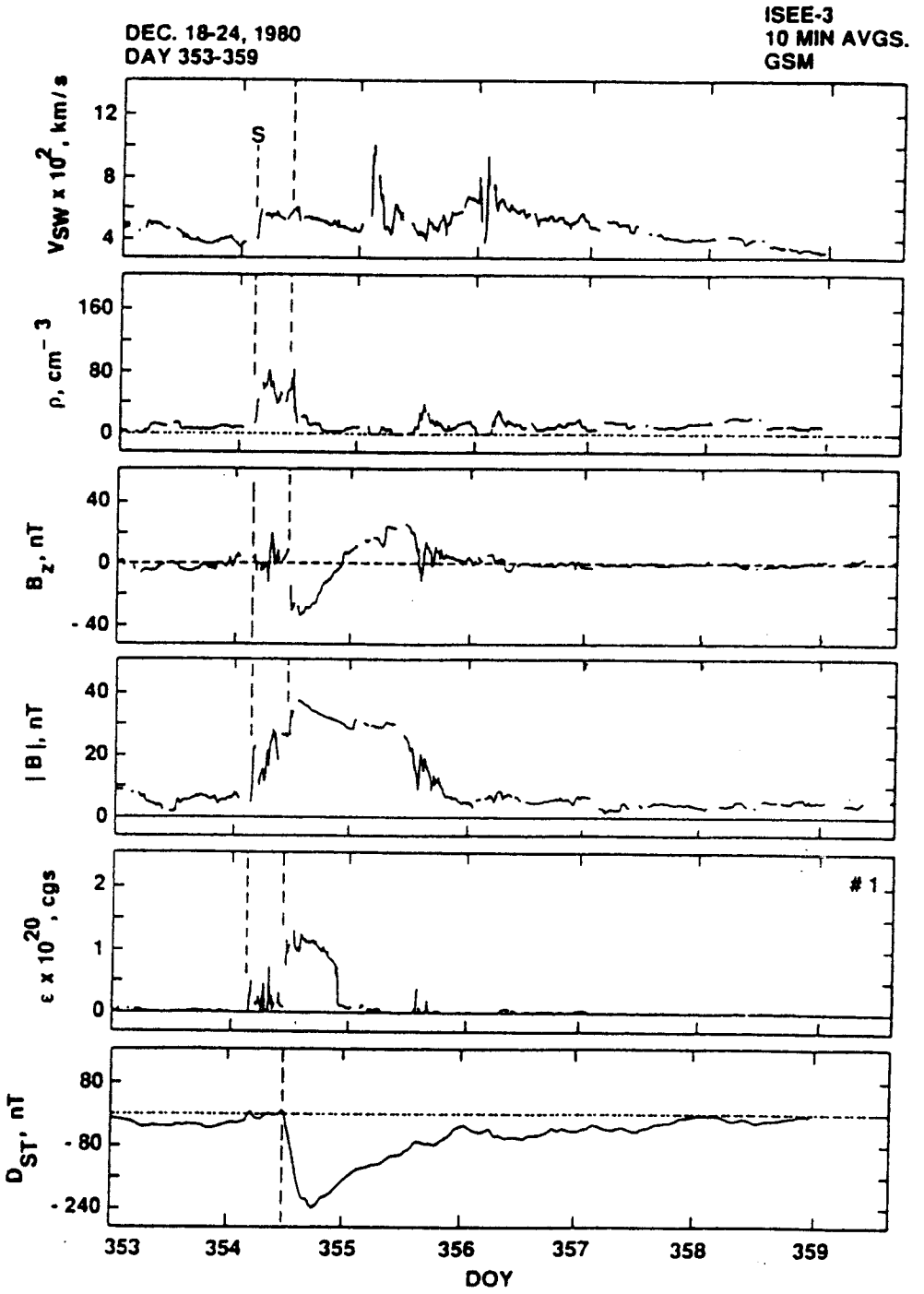
DEC. 18-24, 1980
DAY 353-359
ISEE-3
10 MIN AVGS.
GSM
S
$V_{SW} \times 10^2$, km/s
12
8
4
ρ, cm^{-3}
160
80
0
B_z, nT
40
0
- 40
|B|, nT
40
20
0
$\epsilon \times 10^{20}$, cgs
2
1
0
1
D_{ST}, nT
80
- 80
- 240
353
354
355
356
357
358
359
DOY

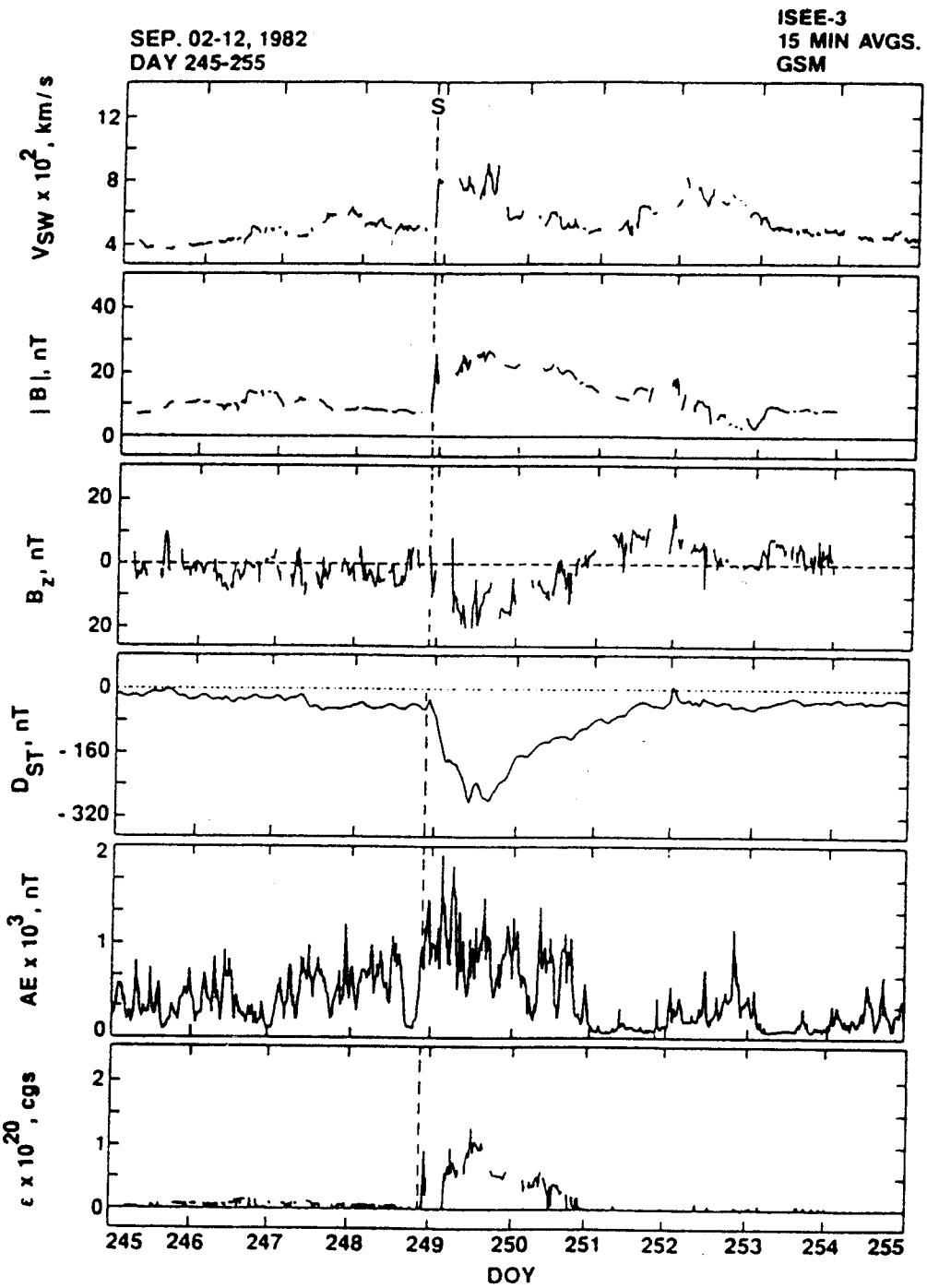
SEP. 02-12, 1982
DAY 245-255
ISEE-3
15 MIN AVGS.
GSM
S
V_{SW} x 10^2, km/s
12
8
4
| B |, nT
40
20
0
B_z, nT
20
0
20
D_{ST}, nT
0
- 160
- 320
AE x 10^3, nT
2
1
0
ϵ x 10^{20}, cgs
2
1
0
245
246
247
248
249
250
251
252
253
254
255
DOY

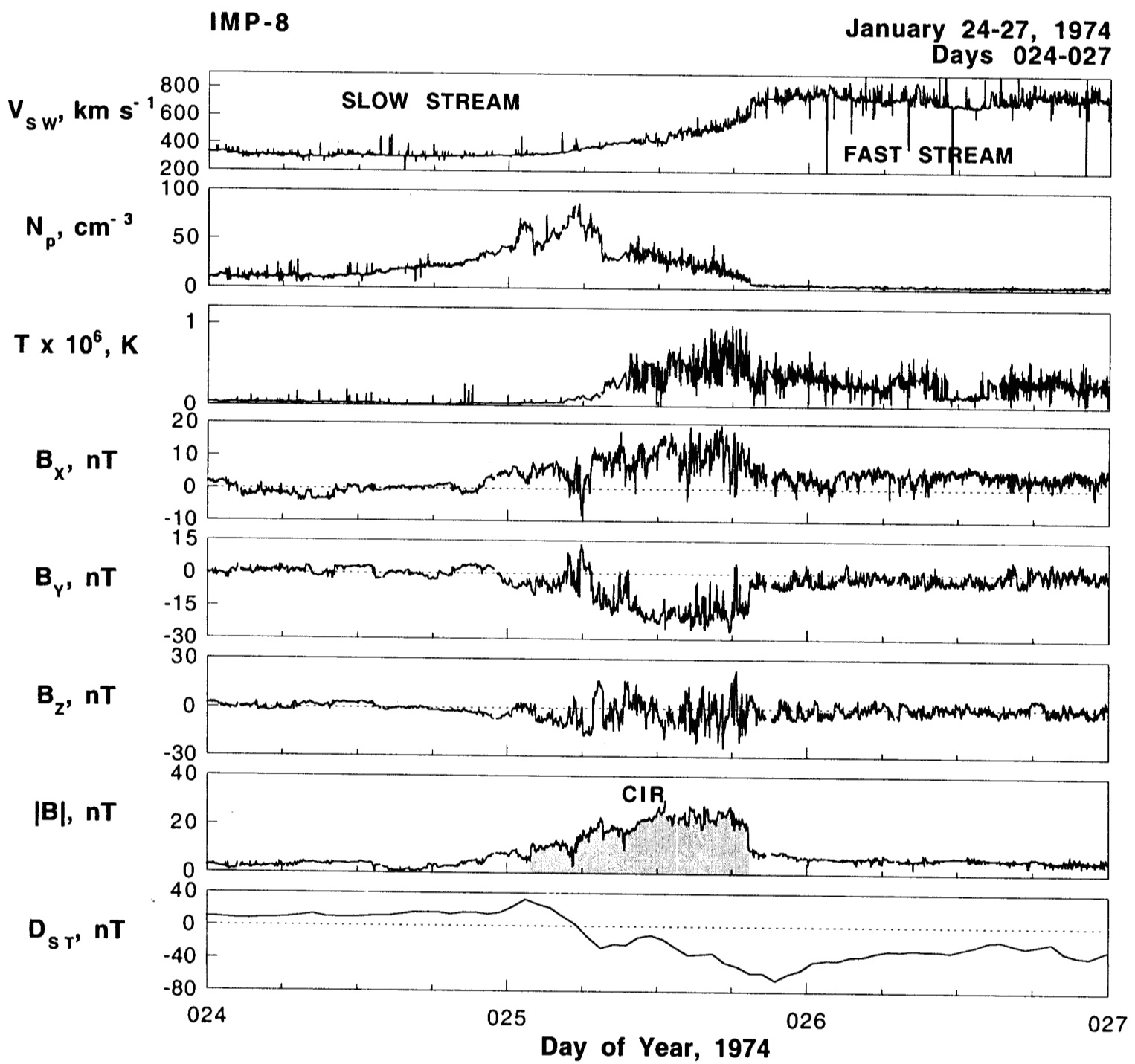
IMP-8
January 24-27, 1974
Days 024-027
V_{SW}, km s^{-1}
800
600
400
200
SLOW STREAM
FAST STREAM
N_p, cm^{-3}
100
50
0
T x 10^6, K
1
0
B_X, nT
20
10
0
-10
B_Y, nT
15
0
-15
-30
B_Z, nT
30
0
-30
|B|, nT
40
20
0
CIR
D_{ST}, nT
40
0
-40
-80
024
025
026
027
Day of Year, 1974

Recovery Phase of a Magnetic Storm

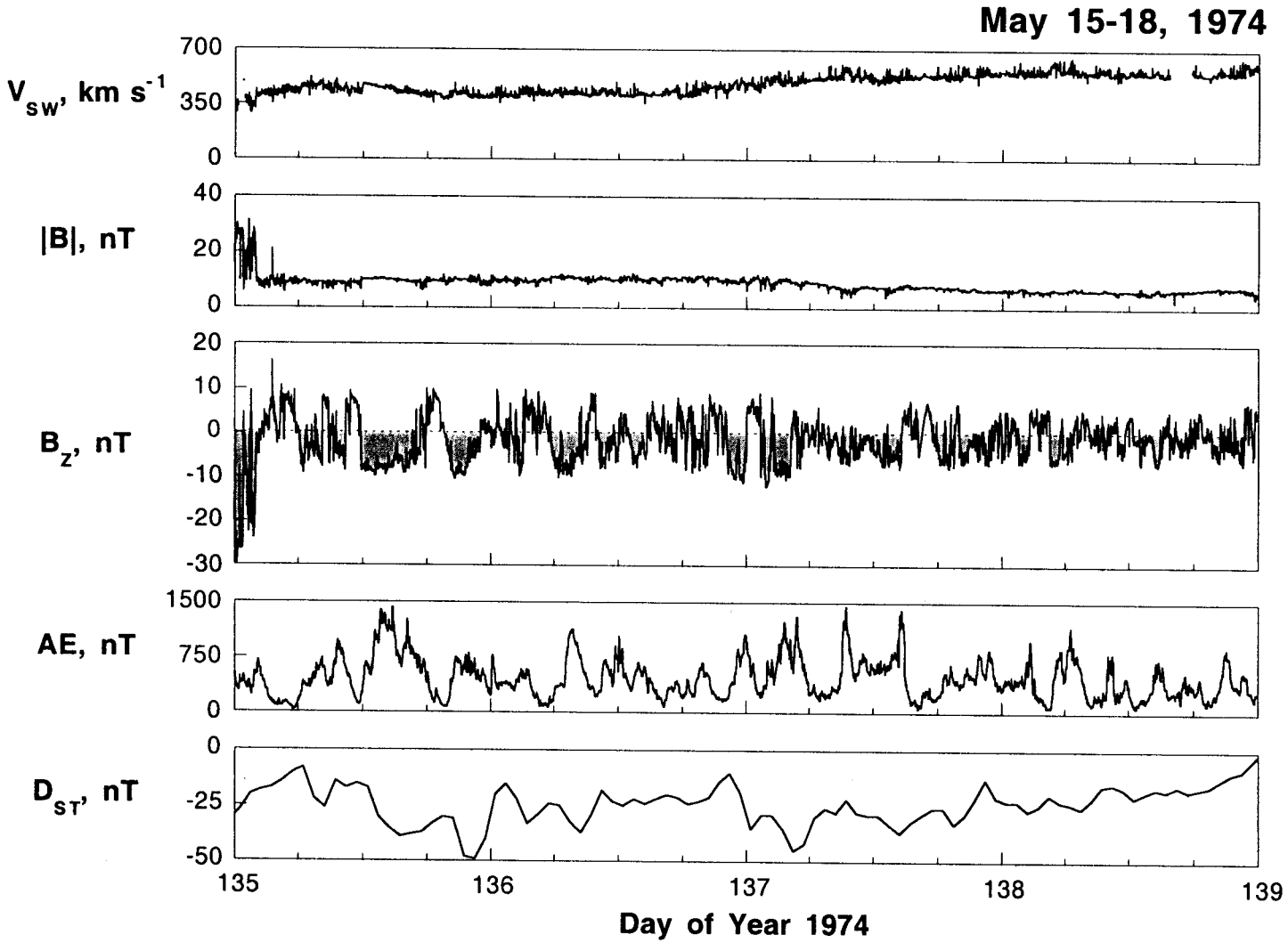

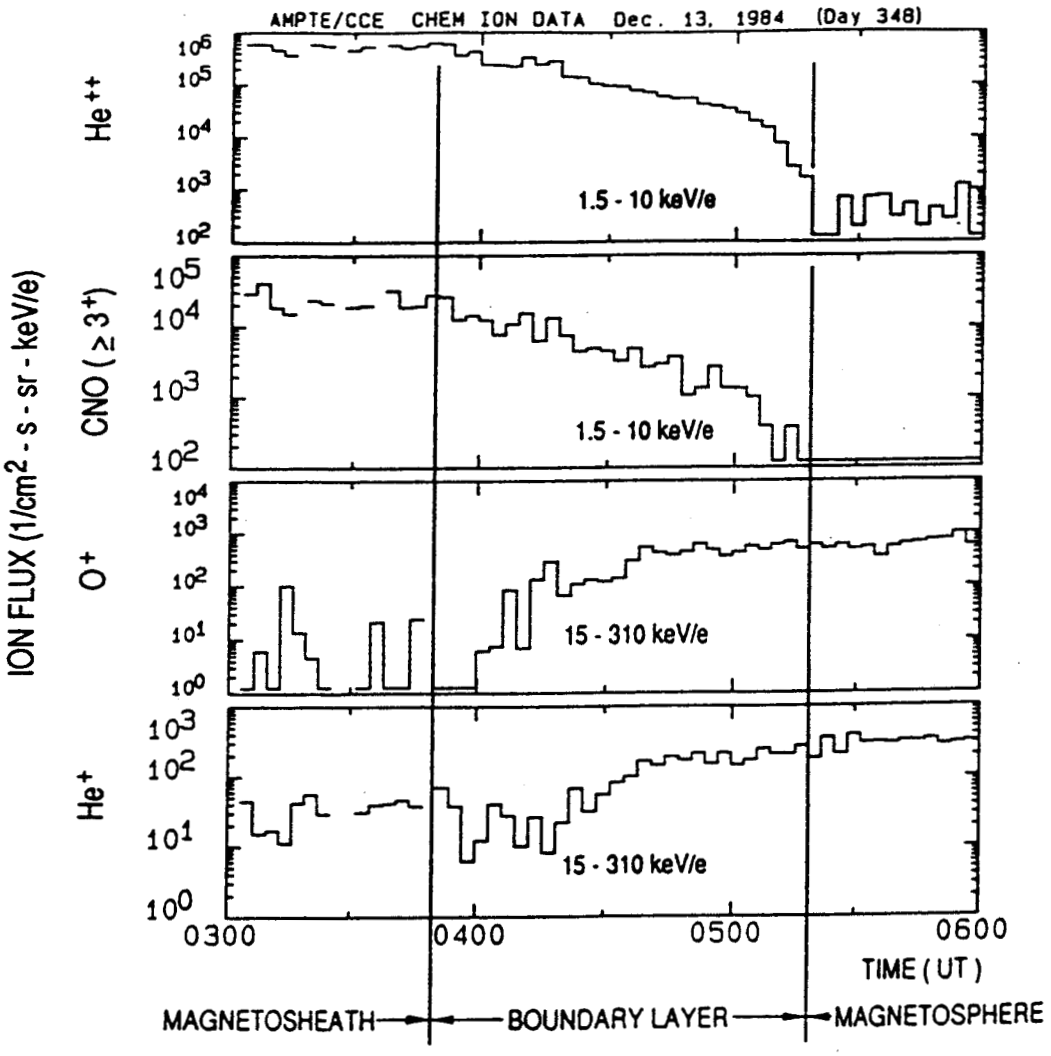
AMPTE/CCE CHEM ION DATA Dec. 13, 1984 (Day 348)
ION FLUX (1/cm² - s - sr - keV/e)
He⁺⁺
1.5 - 10 keV/e
CNO (≥ 3⁺)
1.5 - 10 keV/e
O⁺
15 - 310 keV/e
He⁺
15 - 310 keV/e
0300
0400
0500
0600
TIME (UT)
MAGNETOSHEATH
BOUNDARY LAYER
MAGNETOSPHERE